Available online at www.sciencedirect.com
SCIENCE DIRECT®
Chemical Physics 326 (2006) 478–482
Chemical Physics
www.elsevier.com/locate/chemphys

Dependence of morphology and photoluminescent properties of $GdPO_4:Eu^{3+}$ nanostructures on synthesis condition

Lixin Yu [a,*], Dianchao Li [a], Mingxin Yue [a], Jie Yao [a], Shaozhe Lu [b]

[a] *Key Laboratory of Automobile Materials, Ministry of Education, and College of Material Science and Engineering, Jilin University, 6 West Min-zhu Avenue, Changchun, Jilin 130026, PR China*

[b] *Key Laboratory of Excited State Physics, Changchun Institute of Optics, Fine Mechanics and Physics, Chinese Academy of Sciences, 16 Eastern South-Lake Road, Changchun 130033, PR China*

Received 1 December 2005; accepted 6 March 2006
Available online 10 March 2006

Abstract

$GdPO_4:Eu^{3+}$ nanoparticles, nanowires and nanorods phosphors were successfully synthesized by a hydrothermal method. Their photoluminescent properties were investigated and compared. The results indicated that the one-dimensional nanowires and nanorods were formed as the pH value of precursor solution was 1, 5 and 9, while zero-dimensional nanoparticles were formed for the pH value of 9. The crystallization state of nanoparticles was relative lower and the crystal structure belongs to monoclinic phase for other samples. The charge transfer band (CTB) of Eu^{3+} ions in nanorods (for pH value of 13) clearly blue-shifted in contrast with other samples. The integrate intensity ratio of $^5D_0$–$^7F_2$ to $^5D_0$–$^7F_1$ in nanoparticles increased due to high disorder. The lifetime of $^5D_0$ level of Eu^{3+} in nanoparticles decreased in comparison with other samples and radiative transition rate of $^5D_0$–$\sum_J {}^7F_J$ increased.

PACS: 78.67.Bf; 78.67.Lt; 78.55.−m; 71.10.Li

Keywords: Nanostructures; Luminescence

1. Introduction

It is well known that reduction of particle size of crystalline system can result in remarkable modification of their properties which are different from those of bulk because of high surface to volume ratio and quantum confinement effect of nanometer materials. In 1994, Bhargava et al. reported that radiative transition rate of ZnS:Mn nanocrystals increased five-fold order in comparison with bulk one [1]. Despite this result was strongly criticized later, the studies on nanosized luminescent semiconductor attracted great interests [2–4]. In addition, the research on nanocrystals was critically important for application and fundamental sciences. Rare earth (RE) compounds were extensively applied in luminescence and display device. It is expected that nanosized RE compounds can increase luminescent quantum efficiency and display resolution. To improve luminescent properties of nanocrystalline phosphors and obtain the nanocrystals with different morphology, many preparation methods have been used, such as solid state reactions, sol–gel techniques, hydroxide precipitation, hydrothermal synthesis, spray pyrolysis, laser-heated evaporation and combustion synthesis, etc. [5–8]. Currently, the luminescent RE doped low dimensional nanostructures such as $LaPO_4$:RE nanowires and Y_2O_3:RE nanotubes have also attracted considerable interests [9,10]. Moreover, in an increasing number of cases shape is being of found to be important to the properties of many nanomaterials [11]. Thus, until now, the morphology-control was still focus and strategy of RE doped nanocrystal research.

Lanthanide orthophosphate ($LnPO_4$) belongs to two polymorphic types, the monoclinic monazite type (for La to Gd) and quadratic xenotime type (for Tb to Lu). Due to

* Corresponding author. Fax: +86 431 8502234.
E-mail address: yulixin72@yahoo.com.cn (L. Yu).

0301-0104/$ - see front matter © 2006 Elsevier B.V. All rights reserved.
doi:10.1016/j.chemphys.2006.03.008

its high quantum efficiency, bulk lanthanum and gadolinium phosphate doped Ce^{3+} and Tb^{3+} as an ideal green phosphor in fluorescent lamps, CRT and PDP has been intensively investigated [12–14]. Lanthanide phosphate nanocrystals doped with RE ions have been also reported. In 1999, Meyssamy et al. synthesized $LaPO_4:Eu^{3+}$ and $LaPO_4:Tb^{3+}$ nanocrystals including nanowires (NWs) and nanoparticles (NPs) for the first time and reported their luminescent properties [9]. In 2003, Xu et al. [15] systemically reported the synthesis of lanthanide orthophosphate NWs, and we systematically investigated the photoluminescent properties of Eu^{3+} in $LaPO_4$ nanocrystals [16–19]. Recently, affects of structures of RE doped nanocrystal-hosts on luminescent properties were also reported [20–22]. However, the reports on systematical synthesis and photoluminescent properties of RE ions doped $GdPO_4$ nanocrystals were very rare. Recently, we prepared $GdPO_4:Eu^{3+}$ nanocrystals including NWs, nanorods (NRs) and NPs with a hydrothermal method. Because all samples were synthesized by the same method and compared luminescent properties, we suggested that the comparison of their photoluminescent characteristics should be more compellent.

2. Experiments

2.1. Sample preparation

In the preparation, appropriate amounts of high purity Gd_2O_3 and Eu_2O_3 (1:0.05 in mol ratio) were dissolved into concentrated HNO_3 firstly and appropriate volume de-ionized water was added. Then appropriate volume of $(NH_4)_2HPO_4$ aqueous solution (0.18 M) was added into the above solution. The final pH value was adjusted to 1, 5, 9 and 13 with diluted HNO_3 (1 M) and NaOH solution (4 M), respectively. After well stirred, the milky colloid solution was obtained and poured into several closed Teflon-lined autoclaves and subsequently heated at 130 and 160 °C for 3 h, respectively. The obtained suspension was centrifuged at 4000 rpm for 15 min and supernatant was discarded. Then, the precipitate was dissolved in dilute HNO_3 solution and pH value was adjusted to 1.0. The mixture was stirred for 24 h in order to dissolve $Gd(OH)_3$. The white suspension obtained was centrifuged at 4000 rpm for 15 min. The colorless supernatant concluding by-products was discarded. The precipitation was washed for three times with de-ioned water. The resultant samples were dried at 50 °C at vacuum condition.

2.2. Measurements

Crystal structure, morphology and size were obtained by X-ray diffraction (XRD) using Cu target as radiation resource ($CuK_\alpha = 1.54078$ Å), and transmission electron micrographs (TEM) utilizing JEM-2010 electron microscope.

The excitation and emission spectra at room temperature were measured with a Hitachi F-4500 fluorescence spectrometer. In the measurements of dynamics, a 266-nm light generated from the Fourth-Harmonic-Generator pumped by the pulsed Nd:YAG laser was used as general excitation source. The Nd:YAG laser was with a line width of 1.0 cm^{-1}, pulse duration of 10 ns and repetition frequency of 10 Hz. The dynamics were recorded by a Spex-1403 spectrometer, a photomultiplier and a boxcar integrator and processed by a computer.

3. Results and discussion

3.1. Crystal structure and morphology

Fig. 1 shows TEM images of nanosized $GdPO_4:Eu^{3+}$ samples. It is clear that the morphology greatly changed as the pH value of precursor solution varied from 1 to 13 for the same hydrothermal temperature. As can be seen from TEM, the NRs with large size were formed (labeled with N1) as the pH value of precursor solution was 1, whose width was about 150 nm and length was ~0.5 μm. For pH value of 5, the NWs with high aspect ratios were produced, with the width of 10–20 nm and the length of ~0.5 μm (Labeled with N5). For pH value of 9, the zero-dimensional NPs were formed (labeled with N9). While for pH value of 13, some short NRs were made, whose width was about 5–10 nm and length was about 50 nm. For the same pH value of precursor solution, the morphology and size hardly changed as the hydrothermal temperature varied from 130 to 160 °C. According to Fig. 1, pH value of precursor solution strongly affected the morphology of nanostructures. Yu and co-workers reported that the shape and aspect ratio of tungstate nanostructures were determined by pH value [23]. For $GdPO_4:Eu^{3+}$ nanostructures synthesized by the hydrothermal process, amorphous fine $GdPO_4$ NPs were formed in supersaturated solution firstly, and then they were followed by crystal growth and self-assembly. We suggested that different morphology structures were attributed to the different solubility of $GdPO_4:Eu^{3+}$in precursor solution.

Fig. 2 shows the XRD patterns of $GdPO_4:Eu^{3+}$ nanostructures. It is obvious that the crystallization of N9 was very poor and approached non-crystalline state. The crystal structures of the other samples all belong to monoclinic monazite type (JCPDS No. 84-0920) like the bulk $GdPO_4$ polycrystals prepared with the solid reaction. No additional phase was formed. The crystallization of NPs was very poor and, while for NWs and NRs, was relatively well. Because one-dimensional nanostructures (both NWs and NRs) formed in precursor through self-assembly of NPs, defects will become less and crystallization will become better for one-dimensional nanostructures in the process of self-assembly.

3.2. Excitation and emission spectra

Fig. 3 shows normalized excitation spectra at 609 nm in different $GdPO_4:Eu^{3+}$ samples. In Fig. 3, the wide band

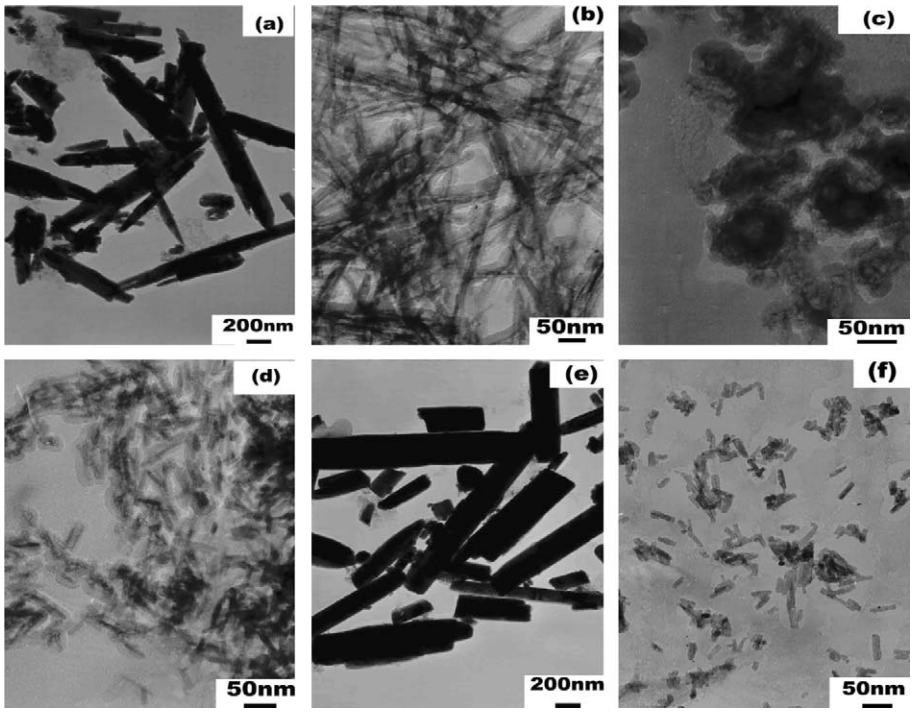

Fig. 1. TEM images of $GdPO_4:Eu^{3+}$ samples. (a) pH 1, $T = 130$ °C; (b) pH 5, $T = 130$ °C; (c) pH 9, $T = 130$ °C; (d) pH 13, $T = 130$ °C; (e) pH 1, $T = 160$ °C; (f) pH 13, $T = 160$ °C.

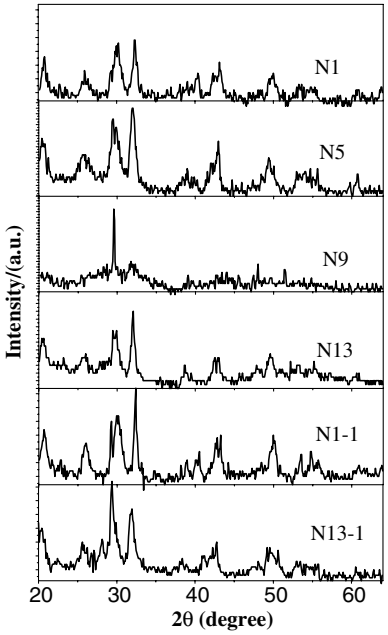

Fig. 2. XRD patterns of $GdPO_4:Eu^{3+}$ samples.

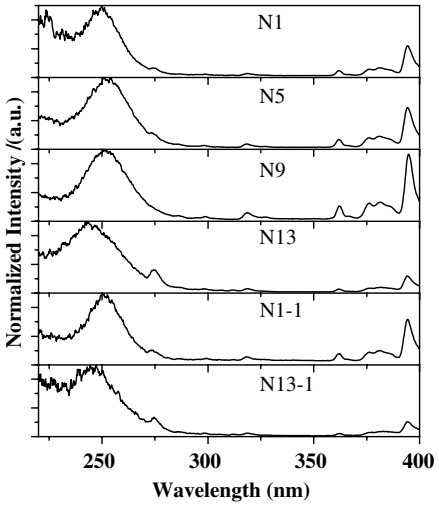

Fig. 3. Normalized excitation spectra of $GdPO_4:Eu^{3+}$ samples ($\lambda_{em} = 609$ nm).

extending from 220 to 300 nm was associated with the charge transfer transition from 2p orbital of O^{2-} ions to the 4f orbital of Eu^{3+} ions, while the sharp lines with the direct excitation of f–f shell transitions of Eu^{3+}. Igrashi et al. reported that in $Y_2O_3:Eu^{3+}$ NPs [24], the CTB blue-shifted as the particle size decreased, and we observed that the CTB of $LaPO_4:Eu^{3+}$ NWs red-shifted intensity in contrast to the NPs and corresponding micrometer samples [16]. According to Fig. 3, the peak locations of the CTB in all samples were determined and listed in Table 1. For N13 and N13-1, the CTB obviously blue-shifted in comparison with other samples. Hoefdraad et al. reported that the position of CTB depends on the Eu^{3+}–O distance [25]. The shorter the Eu–O bond is, the shorter the location of CTB position is. Thereby, we can deduce that the average length of Eu–O bond for N13 and N13-1 is shorter than that for other samples. It implied that the location of CTB of Eu^{3+} in NPs and NWs hardly changed and blue-shifted in NRs. The shoulder at about 275 nm was not

Table 1
The location of CTB of Eu^{3+}, *K*-value and the lifetime of $^5D_0$ level of Eu^{3+} in $GdPO_4$:Eu^{3+} nanocrystals

Sample	N1	N1-1	N5	N9	N13	N13-1
Location of CTB (nm)	249	251	251	252	242	242
K	0.537	0.551	0.571	0.865	0.676	0.715
Lifetime (ms)	1.08	1.02	0.97	0.81	1.03	1.09

associated with the Eu^{3+} ions according to the Eu^{3+} energy level. It originated from the transition from $^8S_{7/2}$ to $^6I_{11/2}$ level of Gd^{3+} ions. This result indicated that the absorptance of Gd^{3+} ions was attributed to luminescence of Eu^{3+} ions, implying that the energy transfer between Gd^{3+} and Eu^{3+} occurred.

Fig. 4 shows the emission spectra of different $GdPO_4$:Eu^{3+} powders at room temperature. The $^5D_0$–^7F_J transitions ($J = 1,2,3,4$) were observed, as labeled in the figure. Among them, the $^5D_0$–$^7F_1$ transitions were the strongest. It is clear that in N9, the emission line of $^5D_0$–$^7F_1$ became broader and Stark splitting of $^5D_0$–$^7F_1$ transitions were hardly observed. In other samples, two Stark splitting lines were observed at least though these lines were entirely separated. In Fig. 4, the intensity ratio (*K*) of $^5D_0$–$^7F_2$ to $^5D_0$–$^7F_1$ in all samples were determined and listed in Table 1. The intensity ratio of $^5D_0$–$^7F_2$ to $^5D_0$–$^7F_1$ varied depending on the morphology of powders. It can be seen that *K* in N9 increased in comparison with that in other samples. As is well known, the $^5D_0$–$^7F_1$ lines originate from magnetic dipole transition, while the $^5D_0$–$^7F_2$ lines from electric dipole one. In terms of the Judd–Ofelt theory [26,27], the magnetic dipole transition is permitted. The electric dipole transition is forbidden and permitted only on condition that the europium ion occupies a site without an inversion center and is sensitive to local symmetry. Subsequently, when Eu^{3+} ions occupy in inversion center sites, the $^5D_0$–$^7F_1$transition should be relative stronger, while the $^5D_0$–$^7F_2$ transition should be relative weaker. The results above indicate that in the $GdPO_4$ host, more Eu^{3+} ions occupied inversion center sites. In N9, the number of Eu^{3+} ions at conversion center sites was less than that in other samples. According to XRD results (Fig. 2), the crystallization of N9 was relative low, indicating the disorder surrounding Eu^{3+} increased, leaded the forbidden transition of $^5D_0$–$^7F_2$ to be further dissolved and emission line became broad.

Fig. 5 shows the normalized decay curves of Eu^{3+} ions at 609 nm emission in $GdPO_4$ hosts. It can be seen that $^5D_0$ level of Eu^{3+} exponentially decayed. The lifetimes of Eu^{3+} were determined by single order fitting and listed in Table 1. It is obvious that the lifetimes of Eu^{3+} in all samples except N9 were nearly same and the lifetime of Eu^{3+} in N9 was shorter than that in other samples. The non-radiative relaxation is a multi-phonon process. Then the lifetime of $^5D_0$ can be expressed as [28,29],

$$\tau(T) = \frac{1}{W_1 + W_{10}(T)}, \tag{1}$$

where W_1 is the radiative transition rate of $^5D_0$–$\sum_J {}^7F_J$, $W_{10}(T)$ is non-radiative transition rate at a certain temperature, *T*. The $^5D_0$ is the lowest excited state and the energy separation between $^5D_0$ and the nearest downlevel $^7F_6$ is as high as $\sim$12,000 cm^{-1}. In this case, non-radiative relaxation processes hardly happen according to the theory of multi-photon relaxation. We have reasons to suppose that the non-radiative transition rate can be neglected in comparison to the total radiative transition rate of $^5D_0$–$\sum_J {}^7F_J$. Thus, the inverse of lifetime at the room temperature equaled to the radiative transition rate of $^5D_0$–$\sum_J {}^7F_J$. The result indicated the radiative transition rate of $^5D_0$–$\sum_J {}^7F_J$ of Eu^{3+} in N9 was higher than that in other samples. According to XRD and spectra results, the disorder of lattice in N9 increased, leading the forbidden transition to be further dissolved and increased the radiative transition rate of $^5D_0$–$\sum_J {}^7F_J$.

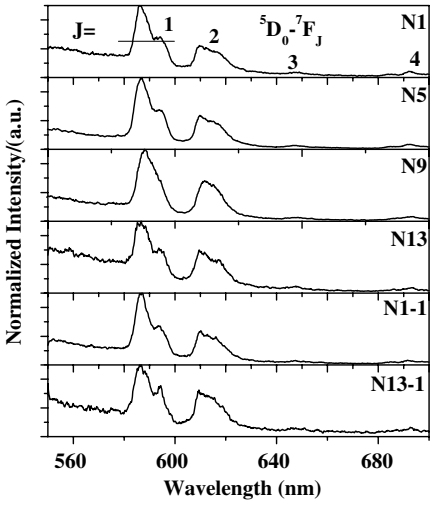

Fig. 4. Emission spectra of $GdPO_4$:Eu^{3+} nanostructures.

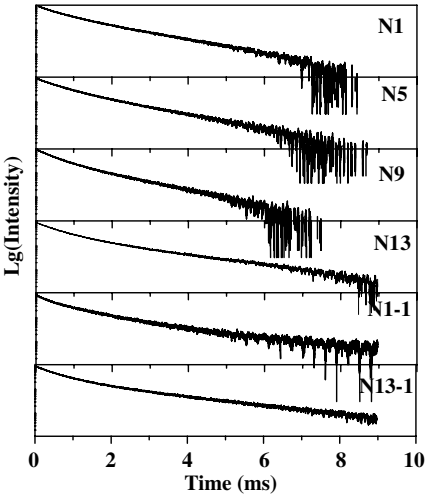

Fig. 5. The decay curves of Eu^{3+} at 609 nm.

4. Conclusions

$GdPO_4$:Eu^{3+} nanostructures with different morphology including NPs, NWs and NRs phosphors were successfully synthesized by a hydrothermal method and characterized by TEM and XRD. Their photoluminescent properties were investigated and compared. The results indicated that the morphology and crystallization strongly depended on the pH value of precursor solution. The one-dimensional NWs and NRs were formed as the pH value of precursor solution was 1, 5 and 9, while zero-dimensional NPs were formed for the pH value of 9. The crystallization state was relative lower for N9 and the crystal structure belongs to monoclinic phase for other samples. The CTB of Eu^{3+} in NRs (N13 and N13-1) greatly blue-shifted. The intensity ratio of $^5D_0$–$^7F_2$ to $^5D_0$–$^7F_1$ in zero-dimensional NPs (N9) increased due to lower crystallization and higher disorder, indicating that more Eu^{3+} ions occupied inverse centers. The lifetime of $^5D_0$ level of Eu^{3+} in N9 decreased in contrast with other samples, indicating that the radiative transition rate of $^5D_0$–$\sum_J {}^7F_J$ of Eu^{3+} increased.

Acknowledgements

The authors gratefully thank the financial supports of Nation Natural Science Foundation of China (Grant No. 10504030 and 10374086).

References

[1] R.N. Bhargava, D. Gallagher, X. Hong, A. Nurmikko, Phys. Rev. Lett. 72 (1994) 416.
[2] Z.W. Pan, Z.R. Dai, Science 291 (2001) 1947.
[3] X.Y. Kong, Y. Ding, R.S. Yang, Science 303 (2004) 349.
[4] X. Wang, J. Zhaung, Q. Peng, Nature 437 (2005) 121.
[5] K. Riwotzki, M. Haase, J. Phys. Chem. B 102 (1998) 10129.
[6] B. Bihari, H. Eilers, B. Tissue, J. Lumin. 75 (1997) 1.
[7] J. Bellessa, S. Rabaste, C. Plenet, J. Mugnier, O. Marty, Appl. Phys. Lett. 79 (2001) 2142.
[8] G.A. Hebbink, J.W. Stouwdam, D.N. Reinhoudt, C. Veggel, Adv. Mater. 14 (2002) 1147.
[9] H. Meyssamy, K. Riwotzki, Adv. Mater. 11 (1999) 840.
[10] C. Wu, W. Qin, G. Qin, D. Zhao, J. Zhang, S. Huang, S. Lu, H. Liu, H. Lin, Appl. Phys. Lett. 82 (2003) 520.
[11] A.S. Barnard, J. Mater. Chem. 16 (2006) 813.
[12] U. Rambabu, D.P. Amalnerkar, B.B. Kale, S. Buddhudu, Mater. Chem. Phys. 70 (2001) 1.
[13] J. Dexpert-Ghys, R. Mauricot, M.D. Faucher, J. Lumin. 69 (1996) 203.
[14] X. Wu, H. You, H. Gui, X. Zeng, G. Hong, C. Kim, C. Pyun, B. Yu, C. Park, Mater. Res. Bull. 37 (2002) 2531.
[15] Y.P. Fang, A.W. Xu, R.Q. Song, J. Am. Chem. Soc. 125 (2003) 16025.
[16] L.X. Yu, H.W. Song, S.Z. Lu, Z.X. Liu, L.M. Yang, J. Phys. Chem. B 108 (2004) 16697.
[17] L.X. Yu, H.W. Song, Z.X. Liu, L.M. Yang, S.Z. Lu, Z.H. Zheng, J. Phys. Chem. B 109 (2005) 11450.
[18] H.W. Song, L.X. Yu, S.Z. Lu, Z.X. Liu, L.M. Yang, Appl. Phys. Lett. 85 (2004) 470.
[19] L.X. Yu, H.W. Song, S.Z. Lu, Z.X. Liu, L.M. Yang, Chem. Phys. Lett. 399 (2004) 384.
[20] O. Lehmann, K. Kompe, M. Hasse, J. Am. Chem. Soc. 126 (2004) 12935.
[21] S. Saha, P.S. Chowdhury, A. Patra, J. Phys. Chem. 109 (2005) 2699.
[22] A. Patra, Chem. Phys. Lett. 387 (2004) 35.
[23] S. Yu, B. Liu, M. Mo, J. Huang, X. Liu, Y. Qian, Adv. Func. Mater. 13 (2003) 639.
[24] T. Igrashi, M. Ihara, T. Kusunoki, K. Ohno, Appl. Phys. Lett. 76 (2000) 1549.
[25] H. Hoefdraad, M. Steglman, G. Blasse, Chem. Phys. Lett. 32 (1975) 1975.
[26] B.R. Judd, Phys. Rev. 127 (1962) 750.
[27] G.S. Ofelt, J. Chem. Phys. 37 (1962) 511.
[28] H.W. Song, J.W. Wang, B.J. Chen, S.Z. Lu, Chem. Phys. Lett. 376 (2003) 1.
[29] H.S. Peng, H.W. Song, B.J. Chen, J.W. Wang, S.Z. Lu, X.G. Kong, J.H. Zhang, J. Chem. Phys. 118 (2003) 3277.